P2.3 LOW-LEVEL WIND JETS IN THE TSUGARU STRAIT BY HIGH-RESOLUTION SATELLITE OBSERVATIONS AND NUMERICAL SIMULATIONS

Teruhisa Shimada and Hiroshi Kawamura
Center for Atmospheric and Oceanic Studies
Graduate School of Science, Tohoku University

Weiming Sha
Atmospheric Science Laboratory
Graduate School of Science, Tohoku University

1 Introduction

The Tsugaru Strait is an international strait of the northwest Pacific, connecting the Japan Sea with the northwestern Pacific Ocean between the Japanese islands (Fig.1). A semi-enclosed bay, called The Mutsu Bay (Fig.2), is open to the Tsugaru Strait through a narrow (10 km) channel on its northeastern side. In stark contrast to high mountain ranges in the Japanese archipelago, the Tsugaru Strait and Mutsu Bay represent the only sea-level passage through the northern Japan (Fig.1).

In summertime, the easterly wind predominates around northern Japan and persistently blows into the area around the Tsugaru Strait. The easterly wind is associated with the high-pressure system over the Sea of Okhotsk, and accompanies cool, wet, low-level clouds and fogs. This wind is known as Yamase (Takai et al., 2006). Low- and sea-level gaps within and adjacent to the Tsugaru Strait promote the formation of strong gap winds. Understanding of such strong winds is especially required not only for air-sea interaction studies but also for marine security. However, no studies have ever tried to present a comprehensive vision of the wind in this study area. This study first investigates the structure and evolution of the easterly winds blowing through the Tsugaru Strait and Mutsu Bay from a case study during 5-10 June 2003, using a high-resolution simulation of a meteorological model as well as satellite and in situ observations.

Corresponding author address: Teruhisa Shimada, Ocean Environment Group, Center for Atmospheric and Oceanic Studies Graduate School of Science, Tohoku University, Japan
Email: shimada@ocean.caos.tohoku.ac.jp

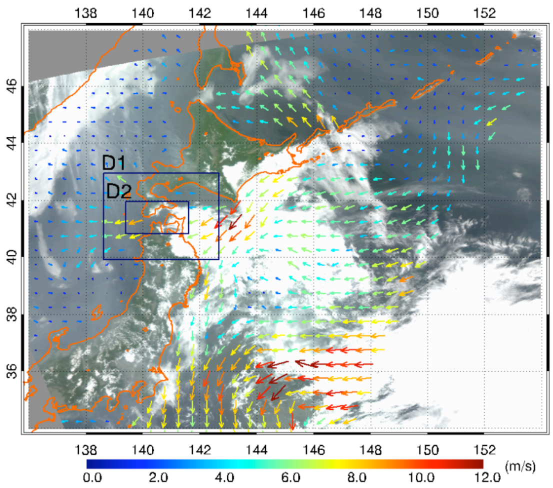

Figure 1 *MODIS visible composite image (R/G/B: channel 1/4/3) at 1216 JST 8 June 2003. Overlaid vectors are ocean surface winds measured by SeaWinds/ADEOS2 at 1033 JST 8 June 2003. Two squares indicated by D1 and D2 are MM5 model domains.*

2 Data and Model simulation

Wind measurements analyzed in this study are acquired by the SeaWinds onboard QuikSCAT and Advanced Earth Observing Satellite 2 (ADEOS2). Wind fields are derived from a RARARSAT ScanSAR image (e.g., Horstmann et al. 2003).

Model simulation efforts in this study are made with the fifth-generation Pennsylvania State University-National Center for Atmospheric Research Mesoscale Model (MM; Grell et al., 1995). We define two model domains with grid sizes of 3 and 1 km (Fig. 1), using two-way interfaces. Thirty-three unevenly spaced sigma levels are used in the vertical, with higher resolution in the boundary layer. Schemes of the MM5 simulation are based on those used in Shimada and Kawamura (2008). A simulation is initialized at 09:00 JST 5 June 2003 and the two domains are integrated to 0900 JST 10 June 2003 during 120 h. We analyze hourly output from the inner domain (Domain 2) (Fig.2).

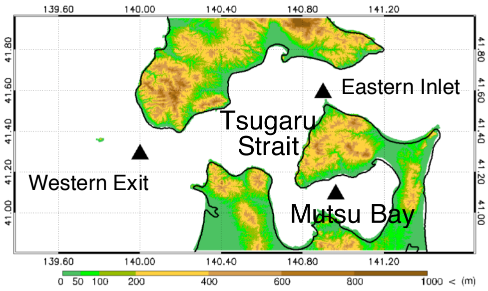

Figure 2 *Map of the study area. Three triangles indicates the location discussed in Fig.6, 8, and 9.*

3 Observational overview

A series of SeaWinds wind measurements during the study period and its full description are presented in Shimada and Kawamura (2007). While the SeaWinds observation frequency is four times per day at most, diurnal variation of the wind jets in the exit of the Tsugaru Strait is apparent. Figure 3 shows a representative example of the strong winds at the most developed stage.

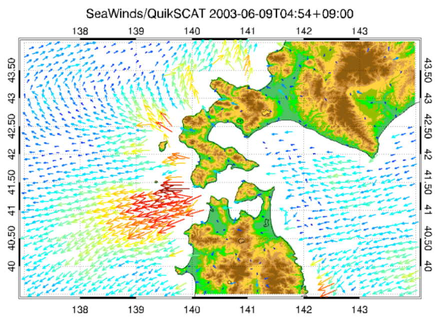

Figure 3 *Ocean surface winds at 12.5-km resolution measured by SeaWinds/QuikSCAT.*

Figure 4 shows a RADARSAT-derived wind field acquired at 0544 JST 9 June 2003. Wind measurements by SeaWinds (Fig. 3) show five wind jets on the western coast of the northern Japan. However, Figure 4 verifies that they are confluent of a few small wind jets. In the west of the Tsugaru Strait, three wind jets with different widths eventually merge into a broad wind jet with 70-km width. Wind maxima are observed at the eastern inlet of the strait and at the center of Mutsu Bay. Detailed descriptions are given in Shimada and Kawamura (2009).

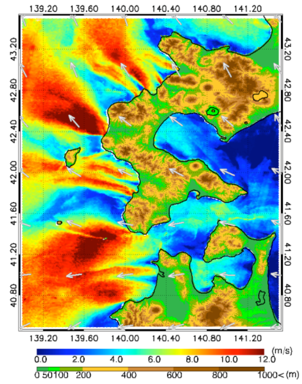

Figure 4 *Wind field derived from a RADARSAT ScanSAR image acquired at 0544 JST 9 June 2003. The arrows with a fixed length represent the wind directions of the GPV (Grid Point Value) data of Japan Meteorological Agency.*

4 Structures and evolution of wind in the Tsugaru Strait and Mutsu Bay

Figure 5 shows simulated 10-m wind fields at 1300 and 0100 JST, averaged hourly during the 4-day period (0900 JST 6 June-0900 JST 10 June). These representative wind fields reveal the structure and diurnal variation of wind within and adjacent the Tsugaru Strait. The wind jet in the west of the strait decreases and shifts to the south during the daytime hours (Fig. 5a). On the other hand, wind speeds in the eastern inlet of the Tsugaru Strait and in Mutsu Bay are high. During the nighttime hours (Fig. 5b), the wind from Mutsu Bay blow toward the western exit. The strong winds from the eastern inlet extend northwestward. As opposed to diurnal variation of wind, the followings are commonly-observed features throughout the study period. Wind enters the study area from the eastern inlet of the strait and the southeastern low-level gap of Mutsu Bay. Winds are strongly blocked in the lee of mountainous area. Additionally, wind speed maxima are seen at the eastern inlet, the center of Mutsu Bay, and the western exit of the strait. From here, we focus on the wind variations at these three locations.

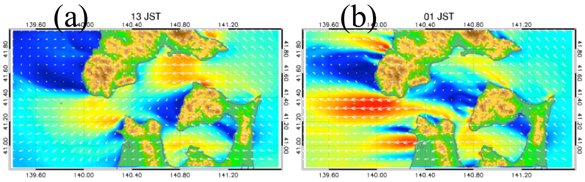

Figure 5 *Simulated 10-m height wind fields at (a) 1300 JST and (b) 01JST averaged hourly from 09:00 JST June 6 2003 to 09:00 JST June 10 2003.*

Figure 6 compares wind timeseries at the three locations to make sure the diurnal variations with different phases. At the western exit, the wind speed generally reaches maximum at around 0000 JST. The only exception is that the wind maximum at around 0000 JST 9 June is not so clear. This may reflects the synoptic variation. Meanwhile, the diurnal variations of winds at the eastern inlet and Mutsu Bay are almost in phase while the wind speeds at the eastern inlet are generally larger than those at the Mutsu Bay location and precede the Mutsu Bay wind by a few hours. The wind speeds at the two locations show a minimum during 0900-1200 JST and a steep rise to maxima at around 1500 JST. Then, the wind speeds gradually decrease to the minimum. It seems reasonable to conclude that there is a time lag between wind variations between eastern and western parts of the strait.

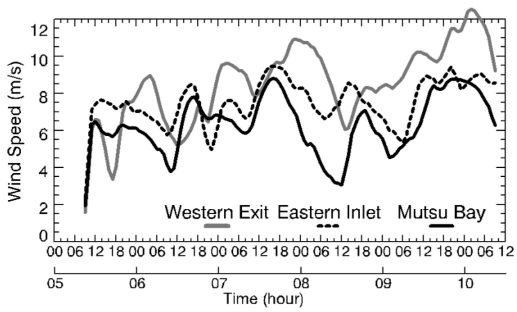

Figure 6 *Simulated wind speed timeseries at the three locations.*

To look into the diurnal cycle of wind, we investigated sea level pressure (SLP) variation, together with air temperature variation (Fig. 7). Generally, contours of air temperatures and SLP are similar. That is, higher SLP appear on the colder air. The SLP contours occlude the narrowest locations (i.e., the three locations mentioned above) all the time. This means that cold air flowing from the east increase SLP. This situation is a typical for gap wind formation [e.g., Steenburgh et al., 1998].

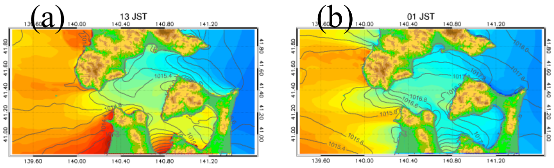

Figure 7 *Simulated 2-m height air temperature (color) and SLP (contours) fields at (a) 1300 JST and (b) 01JST averaged hourly from 09:00 JST June 6 2003 to 09:00 JST June 10 2003.*

Now that air temperature variations are strongly related with wind variations, we compare the air temperature variation at the three locations (Fig. 8). The timeseries of the 2-m air temperature shows obvious diurnal variation, but there are distinct differences between them. Diurnal amplitude of air temperature is smallest (1 ℃) at the eastern inlet. This is because the airflow blowing into the strait from the eastern inlet undergoes the interaction only over the ocean. Air temperature timeseries in Mutsu Bay shows most regular diurnal cycle and the amplitude is largest (2 ℃). This is because the air blowing into the Mutsu Bay receives the heat from the land. Minimum air temperatures at around 0600 JST differ little from those at the eastern inlet (<0.3 ℃). This means that the inflowing air temperatures are almost the same between the eastern inlet and Mutsu Bay. The air temperature at the western exit is highest, reflecting the heat supply from the sea surface during the passage of the strait and air confluence from the eastern inlet and Mutsu Bay. Air temperature variation at the western exit lags behind other two by 6h. This reflects the advection time lag.

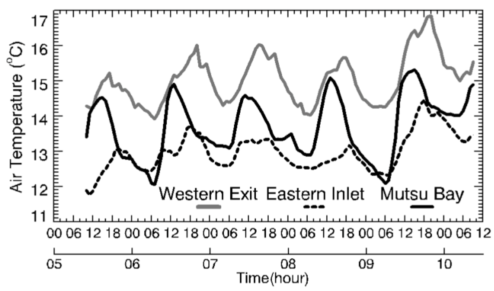

Figure 8 *Simulated 2-m air temperature timeseries at the three locations.*

Finally, we investigate how high the diurnal variations are seen in air temperature structures. Figure 9 shows the time-height diagrams of potential temperature at the three locations. The vertical structures are generally almost the same. This means that the synoptic variations affect the atmospheric structures over the sea surface commonly. Throughout the study period, the atmosphere is stably stratified. However, well-mixed layers are formed below about 500-m height at the three locations, and their potential temperatures vary diurnally in a fairly-regular way. The mixed-layer height is higher at the Mutsu Bay location (~500 m) and the eastern inlet (400-500 m), and lower at the western exit (~300 m). The deep mixed layer reflects the active heating from the surface. The shallower mixed layer may be reflects the expansion fan of atmospheric boundary layer at the western exit.

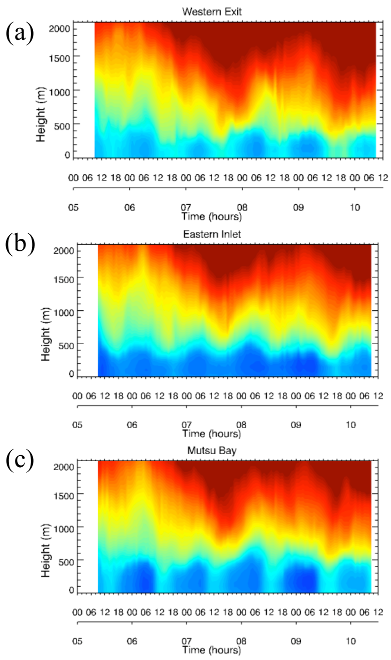

Figure 9 *Time-height diagrams of potential temperature at (a) the western exit, (b) the eastern inlet, and (c) Mutsu Bay.*

5 Summary and Discussion

We have examined and first shed light on the structure and diurnal variations of winds blowing through the Tsugaru Strait and adjacent terrestrial gaps using high-resolution observations and a meteorological model simulation. The event dealt in this study is associated with the cool easterly wind Yamase on 5-10 June 2003. The following conclusions are obtained.

1) It is found that there are two main routes of low-level wind passages. The easterly wind enters the Tsugaru Strait from its eastern inlet and blows toward the western exit. On the other hand, the wind enters Mutsu Bay from its southeast low-level gaps and flow together with the wind from the eastern inlet. The wind speed maxima are observed at the eastern inlet, at the center of Mutsu Bay, and at the western exit of the strait.

2) The low-level easterly winds blowing through the Tsugaru Strait and Mutsu Bay show regular diurnal cycles with a time lag between east and west of the strait. On the east of the strait, the wind speeds increase during the daytime and keep the strong winds during 1500-2100 JST. The maximum wind speeds reaches up to 8-9 m/s at the eastern inlet and at the center of Mutsu Bay. On the west of the strait, wind speeds are minimum during 0900-1500 JST. Then, wind speeds increase from the evening and keep maximum wind speed (12 m/s) during the nighttime hours.

3) The timeseries of the 2-m air temperature show obvious diurnal variation. Air temperature timeseries in Mutsu Bay show most regular diurnal cycle and the amplitude is largest. Diurnal amplitude of air temperature is smallest (1 ℃) at the eastern inlet. The air temperature at the western exit is highest, reflecting the heat supply from the sea surface during the passage of the strait and confluence of wind from Mutsu Bay and the eastern inlet. In the Tsugaru Strait and Mutsu Bay, SLP distributions are consistent with surface air temperature distributions. This suggests that cold air advection in the lower atmosphere determines the SLP, inducing gap-exiting wind.

4) The well-mixed layers are formed below the 500-m height, and the potential temperature of the layers varies diurnally in a fairly-regular way. The diurnal cycles are consistent with surface air temperature. The typical height of the well-mixed layer is higher at the Mutsu Bay location (~500 m) and the eastern inlet (400-500 m), and lower at the western exit (~300 m). Wind speeds are also constant in the well-mixed layers and the heights are consistent with vertically uniform layer of potential temperature (not shown).

5) The satellite and in situ observations verify the above-mentioned simulation results. The 12.5-km SeaWinds wind measurements capture the diurnal variations of winds and the strong wind distribution in the west of the strait. The high-resolution wind field derived from RADARSAT reveals the detailed structure of wind in the strait and strong winds along the western coast. In situ measurements are consistent with the simulated

diurnal variations of wind and air temperature (not shown).

Future work will include the following points. We have to investigate the cause of the diurnal cycle of low-level cold air intrusion toward the study area. Then, it is important to look into the dynamics responsible for the gap winds. The formation mechanisms of these strong winds are remaining issues. Finally, it is important to examine impacts of the alternative strong winds and wakes on regional air-sea interaction.

6 Acknowledgments

We downloaded the SeaWinds/QuikSCAT and SeaWinds/ADEOS2 data from NASA/JPL PO.DAAC. Weather observation station data and AMeDAS data were provided by the Japan Meteorological Agency. Use of MM5 is made possible by the National Center of for Atmospheric Research. This study is partly supported by Exploratory Research Program for Young Scientists of Tohoku University, and by Grants-in-Aid for Scientific Research of Japanese Ministry of Education, Culture, Sports, Science and Technology.

7 References

Grell, G., J. Dudhia, and D. Stauffer (1995), A Description of the Fifth-Generation Penn State/NCAR Mesoscale Model (MM5), *NCAR Tech. Note*, **398**, 122 pp.

Horstmann, J., J. Schiller, J. Schulz-Stellenfleth, and S. Lehner (2003), Global wind speed retrieval from SAR, *IEEE Trans. Geosci. Remote Sens.*, **41(10)**, 2277-2286.

Shimada, T., and H. Kawamura, 2007: Case study of wind jet transition and localized responses of wind wave along the Pacific coast of northern Japan by synergetic use of satellite and in situ observations, *J. Oceanogr.,* **63**, 953-966, 2007.

Shimada, T., O. Isoguchi and H. Kawamura, 2008: Numerical simulations of wind wave growth under coastal wind jet through the Kanmon Strait, *Weather and Forecasting*, Dec, in press.

Shimada, T. and H. Kawamura, 2009: Comparison of wind and wave between high-resolution simulations and operational forecast products: A case of wave distributions under easterly wind jets in the west of the Tsugaru Strait, *Integrated Field Science*, in press.

Steenburgh, W.J., D.M.Schultz, and B.A. Colle, 1998: The structure and evolution of gap outflow over the Gulf of Tehuantepec, Mexico, *Mon. Wea. Rev.*, **126**, 2673-2691.

Takai, H., H. Kawamura, and O. Isoguchi (2006): Characteristics of the Yamase Winds over oceans around Japan observed by the scatterometer-derived ocean surface vector winds, *J. Met. Soc. Japan*, **84(2)**, 365-373.